

# Mixing of North Pacific water masses in the Bali Sea

Andreas Pandapotan<sup>1</sup>, Yuli Naulita<sup>1,\*</sup> and Undang Hernawan<sup>2</sup>

<sup>1</sup> Department of Marine Science and Technology, IPB University, Bogor, Indonesia 16680

<sup>2</sup> Research Center for Oceanography, National Research Center for Oceanography, Jakarta 14430, Indonesia

**Abstract.** As part of the Indonesian Throughflow (ITF) from western route, water masses in the Bali Sea are fed by North Pacific water masses. We examined the mixing strength in the Bali Sea which contributes to reducing the core layer S-max of the North Pacific Subtropical Water (NPSW) from 34.8 – 35 psu in the source region to 34.5 psu in the Bali Sea. Using Thorpe method, we found the mixing strength in the Bali Sea is relatively low. The turbulent kinetic energy dissipation rate ( $\epsilon$ ) of  $O(10^{-11} - 10^{-6}) \text{ WKg}^{-1}$  and density turbulent diffusivity ( $K_\rho$ ) are  $O(10^{-5} - 10^{-3}) \text{ m}^2\text{s}^{-1}$  were similar to typical open ocean values. However, mixing in the eastern region of the Bali Sea is relatively stronger than in the western region. Based on the critical  $Ri \#$ , we found the Thorpe scale ( $L_T$ ) under  $Ri\# < 0.25$  in the eastern region, which is contrary to other parts. It indicated the turbulent mixing was dominantly caused by shear instability. Shear from the strong outflow of ITF towards the Lombok Strait and the reversal northward current in the lower layer forces a strong turbulent layer.

## 1 Introduction

Characteristics of thermocline water masses in the Bali Sea are highly influenced by the Indonesian Throughflow (ITF) which brings the North Pacific Subtropical Water (NPSW) and the North Pacific Intermediate Water (NPIW). Along the western route of the ITF, the core layer of NPSW was greatly reduced but still well-traced of NPIW likes in the Sulawesi Sea, Makassar Strait, and Flores Sea. However, the western route is less dissipative than the eastern route [1-4].

The Bali Sea is close to the Flores Sea and the Banda Sea, we expected the NP water masses would find the same condition in Bali Sea. By using Optimum Multiparameter analysis, Khalisyah *et al.*, [5] found a spatial variation of NP water masses contribution in Bali Sea. The contribution of NPIW is higher (80%) than NPSW (70%) and both water masses have a contrary trend contribution in the west-east direction.

The variation of NP water masses in Bali Sea may influenced by the different hydrodynamics in the eastern and western regions. The strong current in the eastern region is adjacent to the northern part of Lombok Strait where 20% of ITF flows through this strait.

---

\* Corresponding author: [naulita@apps.ipb.ac.id](mailto:naulita@apps.ipb.ac.id)

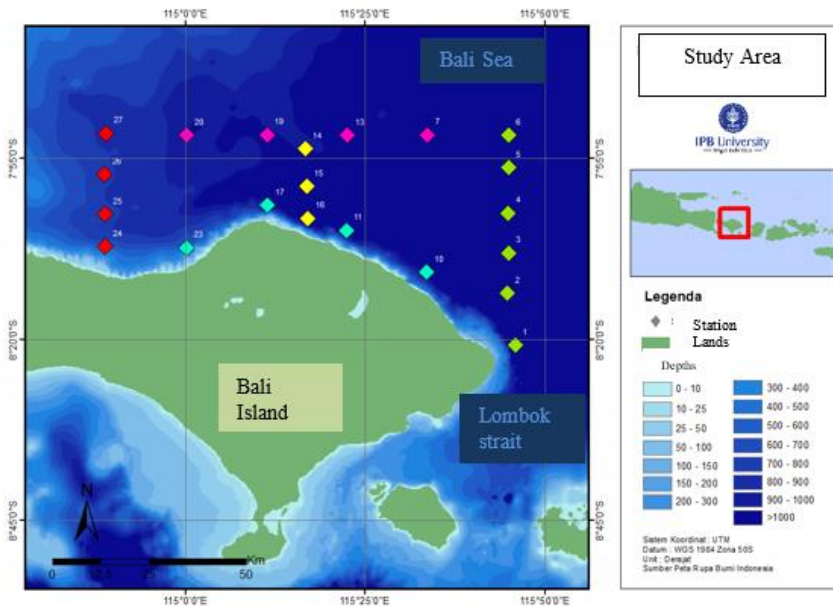
The strong current may induce the mixing process inside the water column. In addition, the Bali Sea has been influenced by Kelvin wave that propagates from the equatorial western Indian Ocean through the Lombok Strait. Kelvin wave causes a reversal current in the water column and deduces the ITF [6-8].

The mixing process in Indonesian seas, including the Bali Sea, is forced by strong tidal and internal waves. The rough topography of the Flores Sea may enhanced the strong mixing but the strength of mixing inside the Bali Sea itself is still unknown. Therefore, we try to estimate the strength of mixing in the Bali Sea through the density overturning that may indicate turbulent mixing.

## 2 Datasets and methods

### 2.1 Datasets

Twenty-one Conductivity Temperature Depth (CTD) stations were conducted in the Bali Sea ( $7.85851^{\circ}$  to  $8.34692^{\circ}$  S and  $114.81494^{\circ}$  to  $115.76413^{\circ}$  E) as shown in **Fig. 1** above. Using CTD Seabird 19 plus, the data were collected from May 21 to June 1<sup>st</sup> 2017, with some CTD Yoyo stations (repeated CTD measurements in one tidal period). The cruise was part of the Ocean Thermal Energy Conversion (OTEC) Expedition using RV Geomarine III.



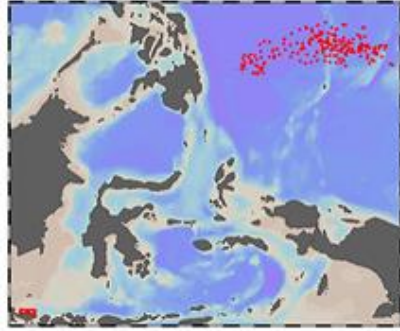


**Fig. 1.** Transects of CTD stations in the Bali Sea (left), and ARGO float stations in the North Pacific Ocean (right).

In addition, we also used CTD data in the NP Ocean obtained from Argo Float (<https://dataselection.euro-argo.eu/>) (**Fig. 1** bottom) as the source of NP water mass. Current, salinity, and temperature data derived from Marine Copernicus (<https://marine.copernicus.eu/>) and tides from the Indonesian Agency for Meteorology, Climatology, and Geophysics (BIG) ([ina-sealevelmonitoring.big.go.id](http://ina-sealevelmonitoring.big.go.id)).

## 2.2 Methods

At first, we examined the stratification, and water mass analysis using TS Diagram, and drew the current pattern in the Bali Sea from Marine Copernicus. For estimating the mixing process, we examined the downcast CTD density profiles indicating the overturning eddy using Thorpe Method. From Thorpe analysis, we gained the Thorpe displacement ( $d_T$ ) calculated from the displacement of density layers in the water column that are in an unstable state (initial condition) to those that have been sorted or have formed static stability. Only  $d_T$  that have passed the Galbraith and Kelley validation [9] will used as the real overturn. Then the length scale of the overturn will be calculated as rms of the real overturns  $d_T$  using the following equation:

$$L_T = \sqrt{\sum_{i=1}^n \langle dTi^2 \rangle} >^{1/2} \quad (1)$$

where  $L_T$  is the Thorpe scale, and  $n$  is the number of samples,  $\langle \rangle$  is averaging process. The  $L_T$  is examined in three layers: the surface mixed layer, the thermocline, and the deep layer. Using the relationship between Thorpe length scale and Ozmidov scale ( $Lo$ ) [10]:

$$Lo = 0.8 L_T \quad (2)$$

we estimate the turbulent of kinetic energy dissipation rate:

$$\varepsilon = Lo^2 N^3 \quad (3)$$

$N^2$  = the Brunt-Väisälä frequency =  $(-\frac{g}{\rho} \frac{\partial \rho}{\partial z})$ , where  $\rho$  is the background water density,  $\partial \rho$  is the density gradient to depth, and  $g$  is the acceleration due to gravity ( $9.79423 \text{ m}^{-2}$ ).

The vertical eddy diffusivity values obtained through the following equation from:

$$K\rho = \Gamma \varepsilon / N^2 \quad (4)$$

$\Gamma$  is the mixing efficiency (0.2) from Osborn [11].

### 3 Results and discussions

#### 3.1 The stratified of the Bali Sea

The Bali Sea shows stratification in temperature and salinity. In all areas, the thickness of the mixed surface layer and thermocline layer is almost the same, about 25 to 60 m and 100-125 m respectively (**Fig. 2**). Inside the stratified water column, sometimes one can find the strong internal wave indicated by isopycnal displacement. In the case of this CTD observation time (May 2017), the occurrence of an internal wave is quite weak but previous studies showed strong internal waves in the Bali Sea where internal solitary waves (ISW) are frequently observed [12, 13]. From acoustic current measurement, [12] found the amplitude of ISW up to 45 m, generated a strong northward current  $\sim 0.8 \text{ ms}^{-1}$ .

The static stability background of the Bali Sea water column is revealed by Brunt-Vaisala frequency ( $N^2$ ) profiles. The  $N^2$  profiles show a similar pattern, where the  $N^2$  high values were found in the thermocline layer. Pond and Pickard [14] stated that the high  $N^2$  values in the thermocline layer are due to the presence of the pycnocline layer. The pycnocline is a layer where the density gradient increases sharply with depth (pressure), leading to increased static stability in the water column. However, the western transect exhibits a bit smaller  $N^2$  values than the other transects. This indicates that the thermocline layer in the western transect has static instability characteristics which relatively easier to be disturbed by the strong internal wave.

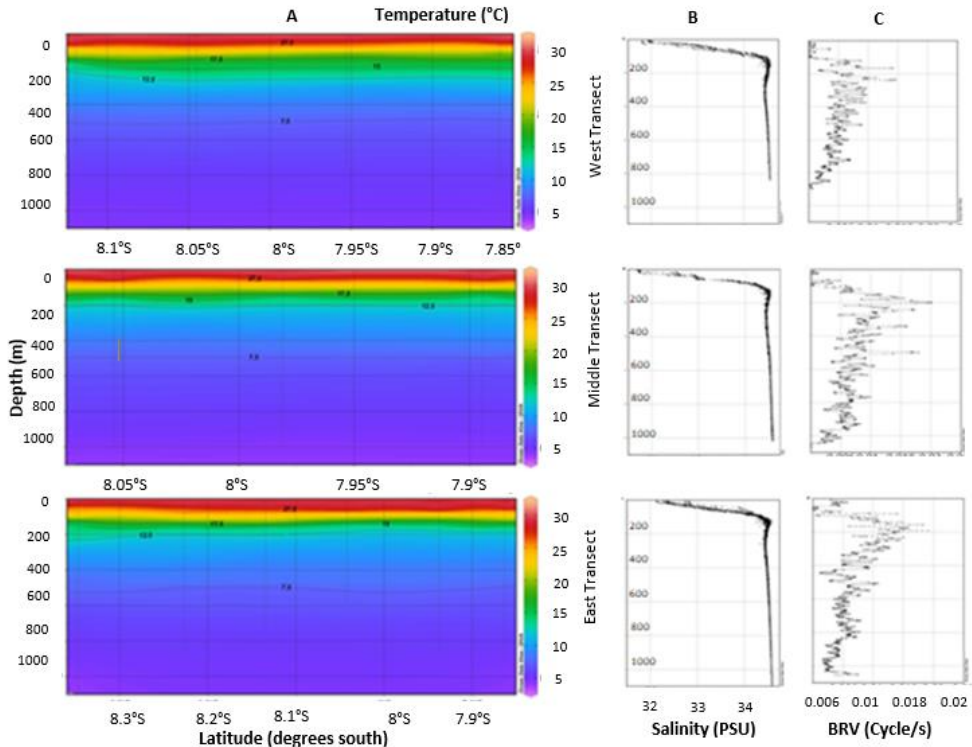


**Fig. 2.** Cross-section of temperature (A); Salinity profiles (B); and Brunt-Väisälä frequency (N) profiles (C) in the Bali Sea.

### 3.2 Water mass characteristics

Low-density water with relatively high temperatures and low salinity is found in the surface mixed layer. This characterized the Java water mass [15]. Inside the thermocline layer, we still can trace the remnant of the core layer of S-max (NPSW) and the S-min of NPIW. The S-max value of NPSW is about 34.52-34.57 psu, temperature 16.02-17.63°C, and lies at 119-145 m depth. The S-min value of NPIW is about 34.32-34.34.44 psu, temperature 11.72-11.73 °C, at a depth of 205-286m.

The characteristics of NPSW and NPIW water masses found in the Bali Sea differ from those in the NP Ocean. The S-max value of NPSW in the NP Ocean is about 34.8-35.2 psu and the S-min of NPIW is about 34.1-34.5 psu [16]. The decrease in salinity is attributed to the transformation of water masses along the west route of ITF (Sulawesi Sea and Makassar Strait) before they enter the Indian Ocean [17].

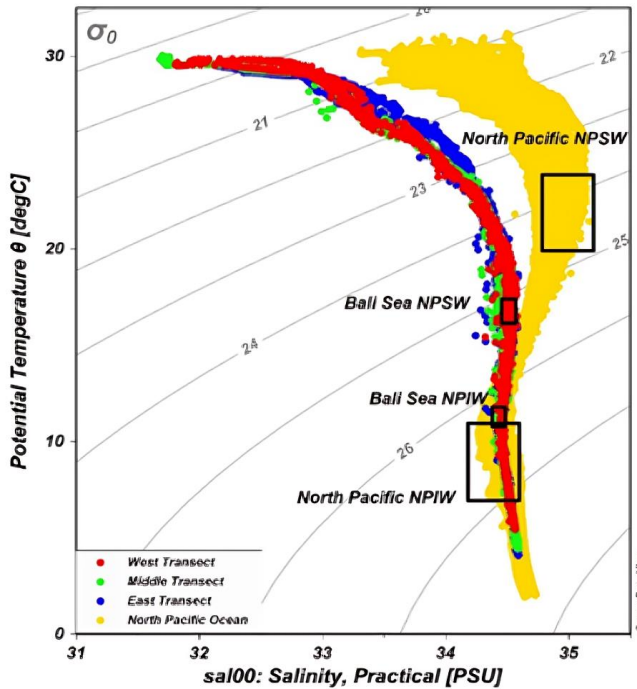


**Fig. 3.** TS Diagram of NPSW and NPIW in the North Pacific Ocean and in the Bali Sea.

### 3.3 Hydrodynamics of the Bali Sea

Hydrodynamics of the Bali Sea is strongly affected by regional monsoon forcing and ITF. Contrast current's strength in the western and eastern regions of the Bali Sea clearly seen from **Fig. 4**. The left figure shows the current from Marine Copernicus at the surface layer (0.5 m) and the right figure reveals the current pattern at the thermocline layer (150 m) at the time of CTD observation. The monsoonal current flows to the Java Sea (0.12-0.18m/s) at the surface layer while the strong ITF outflow (0.33 – 1.09 m/s) goes to Lombok Strait. The strength of the current decreases with depth, at 150m the speed decreases to 0.09-0.29m/s at the western region. As current can induce turbulence in the ocean, the dynamic may influence the strength of the mixing process in the Bali Sea.

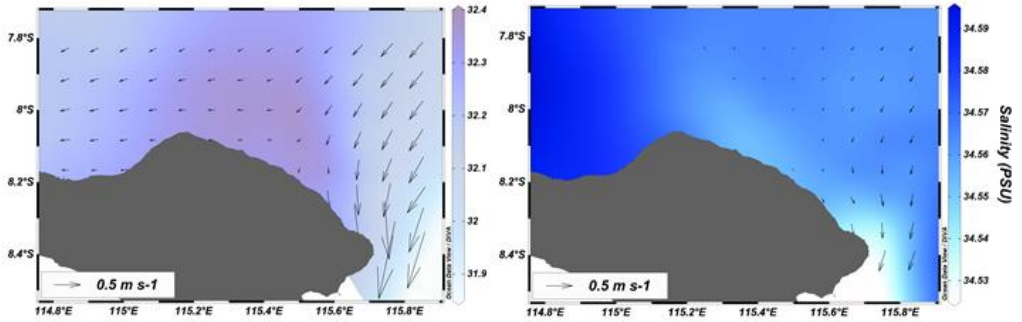


**Fig. 4.** Current overlaid with salinity at the surface (left) and the thermocline depth (right) the Bali Sea in May 5<sup>th</sup> 2017.

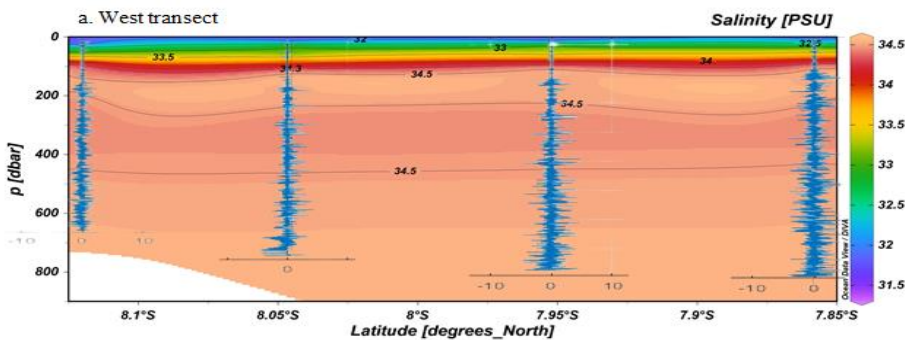
### 3.4 The overturn regions in the Bali Sea

Overturn regions detected from density profiles may indicate the overturning eddy. From Thorpe analysis, we found the size of overturn regions in the Bali Sea as shown in **Table 1**. The overturn regions mostly are small, the size is up to 7 m. The relatively large overturn region (Thorpe displacement  $d_T > 5$  m) was found at the deep layer and less at the thermocline layer. It is related to less stratified water inside the deep layer ( $N = 0.0001-0.02$  cycle  $s^{-1}$ ).

**Table 1.** Distribution of Thorpe displacement in the Bali Sea.

Layer	Thorpe displacement ( $d_T$ )						
	$\pm 1$ m	$\pm 2$ m	$\pm 3$ m	$\pm 4$ m	$\pm 5$ m	$\pm 6$ m	$\pm 7$ m
Mixed layer	331	100	48	24	19	3	0
Thermocline layer	1541	293	55	16	15	6	0
Deep layer	17066	7708	3236	1430	720	332	103

The spatial variation of  $d_T$  in the Bali Sea is revealed in **Fig. 5**. Thorpe displacement  $d_T$  in the western region of the Bali Sea is relatively smaller than in the eastern region, and the largest ones are in the middle. Thorpe displacement in the mixed layer is small and tends to become larger in the deep layer. The salinity distribution background in **Fig. 5** shows that no correlation between the size of overturn regions and the position of NP water masses inside the Bali Sea.





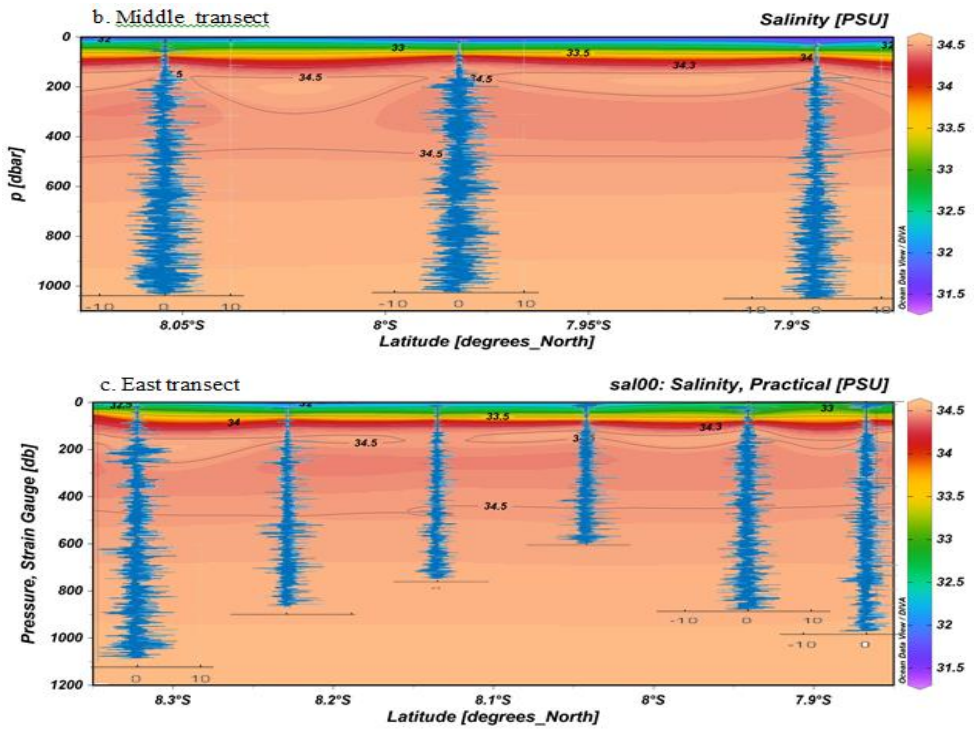


**Fig 5.** Cross-section of salinity overlaid with Thorpe displacement profiles, in the western region (a), middle (b) and the eastern region (c) of the Bali Sea.

To find the contribution of tides to the mixing process in the Bali Sea, we plotted the surface tides at the time of Yoyo CTD station 6 (**Fig. 6**). There were nine CTD profiles in one tidal cycle on May 23, 2017. The Bali Sea experiences semidiurnal tides with two different heights of high tide.

Expected internal tides showed weak isopycnal displacement of  $22.00\text{--}26.00 \text{ kg}\cdot\text{m}^{-3}$  at the interface between the mixed layer and the thermocline layer, as well as by the isopycnal  $27.00 \text{ kg}\cdot\text{m}^{-3}$  at 600 m depth. During high tide, the deeper water is pushed up to a shallower depth in the morning time (08.00–12.00 am), while during low tide, the water is pushed down to a deeper layer in the afternoon time (3.00–5.00 pm). The clear evidence of internal waves in the Bali Sea can be seen through satellite images or current direct measurements. Using sentinel-1 satellite observation, [13] found the internal wave propagation in the Bali Sea, in April 2021. From acoustic current measurement, [12] found ISW events in the Bali Sea suggesting that waves emanated from the Lombok Strait. The wave is relatively small and the  $d_T$  over one tidal cycle has similar values, up to 5 m at the deep layer. The  $d_T$  at the surface is about 3 m and decreases to 1.5 m to 2 m with increasing depth. There is no significant  $d_T$  size between high tides and low tides.

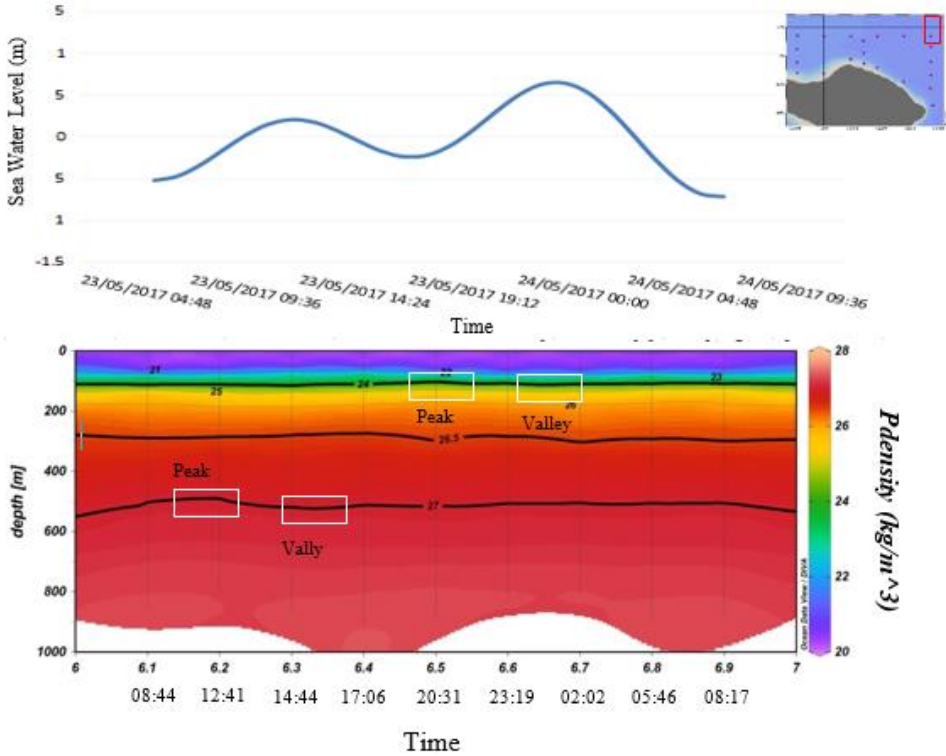


**Fig. 6.** Cross-section of density overlaid with Thorpe displacement  $d_T$  at Yoyo station 6 of the Bali Sea. Inset: Semidiurnal tides of Bali Sea.

### 3.5 Estimation of the turbulent mixing

Ocean mixing may be induced by various mechanisms such as wind and wave at the surface layer, breaking internal waves inside the stratified water column, or double diffusion at interleaving water mass. The strength of mixing can be estimated through the values of the turbulent kinetic energy dissipation ( $\epsilon$ ) and density turbulent diffusivity ( $K\rho$ ). The  $\epsilon$  value represents the amount of energy dissipation released during turbulence, while  $K\rho$  indicates the magnitude of diffusivity for transferring energy during turbulence. The distribution of  $\epsilon$  and  $K\rho$  values in the western, middle, and eastern parts of the Bali Sea is presented in **Fig. 7**. The  $\epsilon$  and  $K\rho$  values are relatively low, with  $\epsilon$   $O(10^{-11}-10^{-6})$   $Wkg^{-1}$  and  $K\rho$   $O(10^{-5}-10^{-3})$   $m^2s^{-1}$ .

However, there is a significant difference with the eastern region of the Bali Sea. Spatial variation of  $\epsilon$  and  $K\rho$  are represented by station 24 in the western region, station 15 in the middle, and station 6 in the eastern region of the Bali Sea (**Fig. 7**). The strong ITF outflow into Lombok Strait plays an important role in inducing turbulent mixing (**Fig. 7** above). Strong ITF outflow can generate strong shear which causes a turbulence layer. In May, [18] stated that the lower layer of the Lombok Strait occurs maximum northward flow. This flow is likely to enter the Bali Sea, causing shear instability. The northward flow is in response to the passage of semi-annual Indian Ocean Kelvin wave. The relation between shear and



turbulence in the eastern region is clearly seen in the scatterplot of the Thorpe Scale,  $L_T$ , with Richardson number ( $Ri\#$ ) as shown in **Fig. 8**.

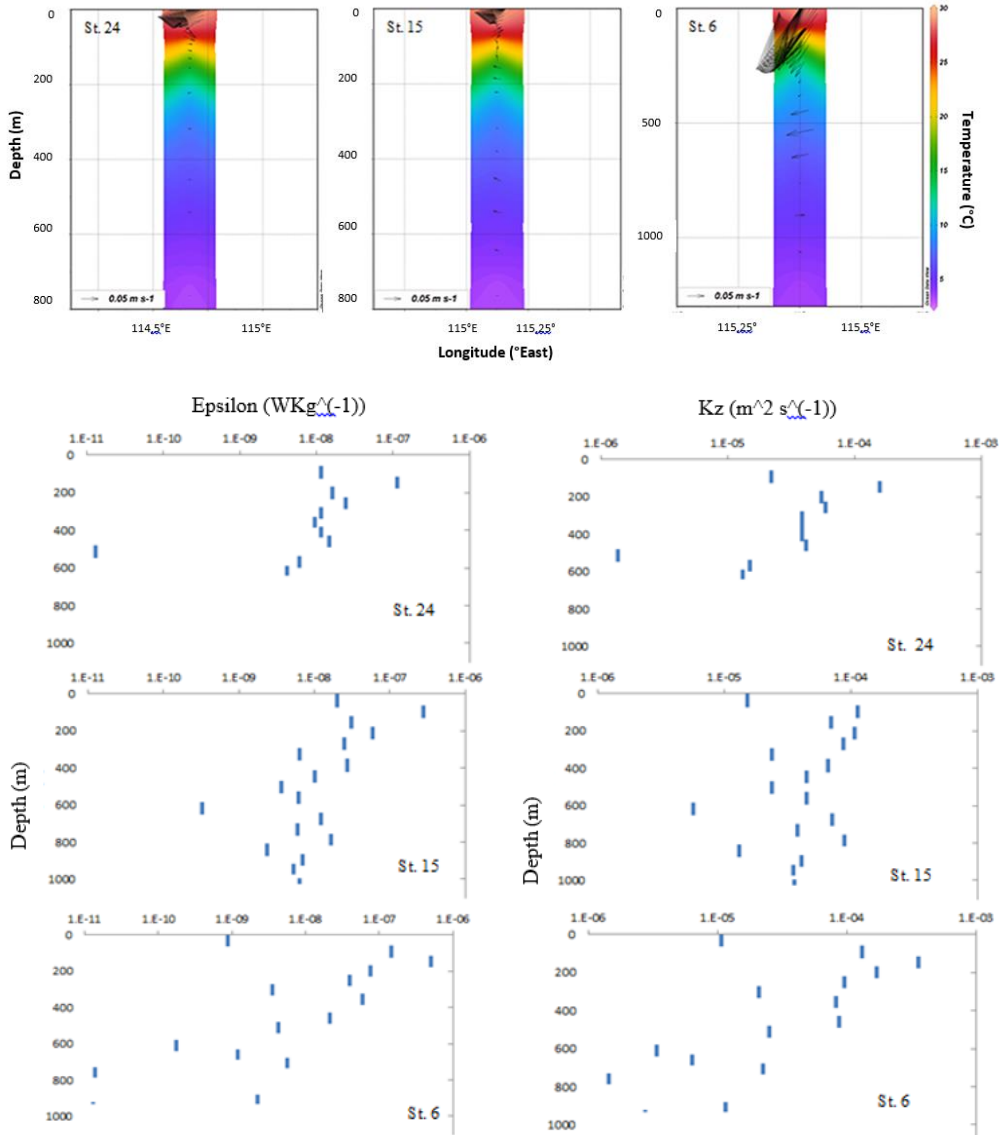


**Fig 7.** Current profiles (above), the turbulent kinetic energy dissipation ( $\epsilon$ ) (left below) and density turbulent diffusivity ( $K\rho$ ) (right below) at station 24, station 15 and station 6 of the Bali Sea.

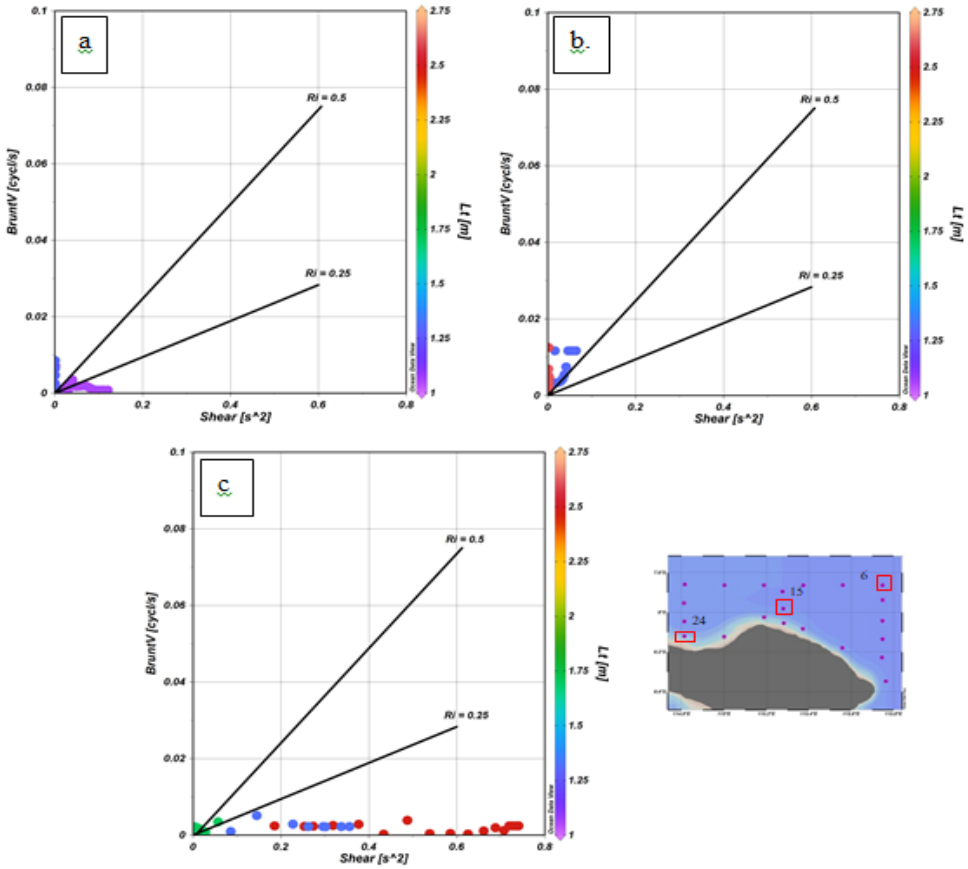


**Fig. 8.** Scatter plot of Thorpe Scale ( $L_T$ ) on shear, buoyancy frequency, and Richardson number (Ri) at station 24 (a), station 15 (b) and station 6 (c) in the Bali Sea.

The critical value of Ri is 0.25, the role of shear instability in turbulent mixing occurs at  $Ri < 0.25$ . On the other hand,  $Ri > 0.25$  indicates well-stratified water or stable water masses. Most of the  $L_T$  in the eastern region is under  $Ri < 0.25$  that is in **Fig. 8**. The same situation was also found in the Lombok Strait, where shear instability associated with internal wave breaking is the main forcing of turbulent mixing [19]. Interestingly, a different situation occurs in the middle of the Bali Sea, where the Thorpe scale is above the critical Ri, even the  $Ri = 0.5$ . Meanwhile, in the western region, the  $L_T$  is on both sides of the critical Ri. More detailed observations are needed to find out the mechanism that drives turbulent mixing.

## 4 Conclusion

During the CTD observation time in late May, the mixing process in the Bali Sea is relatively low. At the same time, indication of the presence of internal waves through water mass distribution was weak. The turbulent kinetic energy dissipation rate ( $\epsilon$ ) of the order  $10^{-11} - 10^{-6} \text{ W Kg}^{-1}$  and density turbulent diffusivity ( $K_\rho$ ) are  $O(10^{-5} - 10^{-3}) \text{ m}^2\text{s}^{-1}$ . There is a spatial variation of turbulence strength in the Bali Sea. The turbulent mixing in the eastern region is relatively stronger, associated with strong ITF outflow and reversal northward current at below the thermocline layer. Indirectly, it is indicated that the propagation of internal waves from the Lombok Strait contributes to the mixing process in the Bali Sea.

## References

1. A.L. Gordon, R.A. Fine, *Nature*, **379**(65610), 146-149 (1996)
2. A. Purwandana, Y. Cuypers, P. Bouruet-Aubertot, T. Nagai, T. Hibiya, A.S. Atmadipoera, *Prog. Oceanogr.* **184**, 102312 (2020)
3. Y. Naulita, *J. Ilmu dan Teknologi Kelautan Tropis*, **8**(1), 345 – 355 (2016)
4. T. Nagai, T. Hibiya, F. Syamsuddin, *Geophys Res Lett* **48** e2020GL091731 (2021)
5. P.V. Khalishah, Y. Naulita, U. Hernawan, *IOP Conf. Series: Earth and Environmental Science* **1251** 012039 (2023)
6. D. Sutanto, L. Mitnik, Q. Zheng, *Oceanography* **18**(4), 80-87 (2005)
7. J. Sprintall, S.E. Wijffels, R. Molcard, I. Jaya, J. Geophys. Res. **114**(C7), 1-19 (2009)
8. F. Syamsudin, N. Taniguchi, C. Zhang, A.D. Hanifa, G.Li, M.Chen. H. Mutsuda, Z.N.Zhu, X.H. Zhu, T. Nagai, A. Kaneko, *Geophys Res Lett.*, **46**(17-18), L10475-10483 (2019)
9. P.S. Galbraith, E. Kelly, *J. Atmos. Ocean Tech.* **13**, 688-702 (1996)
10. T.M. Dillon, *J. Geophys. Res.* **87**(C12), 9601-9613 (1982)
11. T.R. Osborn, *J Phys Oceanogr.* **10**, 83–89 (1980)
12. A. Purwandana, Y. Cuypers, D. Surinati, R. Iskandar, P. Bouruet-Aubertot, *Regional Studies in Marine Science* **57**, 102764 (2023)
13. G. Harsono, B. Purwanto, R.A.G Gultom, T.Puliwarna, J. Setiyadi, K. Ando, M. Cobral. *Ind. J. Maret. Sci.* **26**(4), 282-297 (2021)
14. S. Pond, G.L. Pickard. *Introductory Dynamical Oceanography*. Ed ke-2. Oxford: Pergamon Press. (1983)
15. A.L. Gordon, J. Sprintall, H.M. Van Aken, D.Susanto, S. Wijffels, R. Molcard, A. Ffield, W. Pranowo, S. Wisasantosa, *Dyn. Atmospheres Oceans* **50**(2), 115-128 (2010)
16. K. Wyrтки, *Physical Oceanography of the Southeast Asian Waters*, **2**, 195 (1961)
17. S. Janet, Arnold L. Gordon, Ariane Koch-Larrouy, Tong Lee, James T. Potemra, Kandaga Pujiana, and Susan E. Wijffels, *The Indonesian Seas and Their Role in The Coupled Ocean-Climate System. Nature geoscience* **7**, 487-492 (2014)
18. S.L. Hautala, J. Sprintall, J.T. Potemra, J.C. Chong, W. Pandu, N. Bray, A.G. Ilahude, *J. Geophys.res.* **106**(19527) (2001)
19. Y. Naulita, N.M.N. Natih, Nabil, *IOP Conf. Series: Earth and Environmental Science* **944** 012067 (2021)